Journal of Applied Sciences

ISSN 1812-5654

science alert

ANSInet
an open access publisher
http://ansinet.com

Journal of Applied Sciences 7 (16): 2241-2251, 2007
ISSN 1812-5654

Hydrogeological Framework and Groundwater Modeling of the Sujas Basin, Zanjan Province, Iran

[1]A. Taheri Tizro, [2]A.E. Fryar and [1]K. Akbari
[1]Department of Water Engineering, Razi University, Kermanshah, Iran
[2]Department of Earth and Environmental Sciences, University of Kentucky,
101 Slone Building, Lexington, KY 40506-0053

Abstract: Due to overdraft conditions appearing in most of Iran, management strategies are gaining importance in groundwater studies. Although regional geologic, tectonic and geophysical investigations of the Sujas basin in northwestern Iran have been carried out by the Geological Survey of Iran and water organizations, no conceptual or mathematical modeling of the hydrogeology of the area has been conducted. In this study, detailed local geological, geophysical and hydrogeological investigations were carried out to delineate the architecture of different subsurface geological horizons using lithologs and vertical electrical sounding data. The geological and geoelectrical studies have revealed the existence of a deeper aquifer overlain by relatively impermeable Pleistocene beds of considerable thickness in the eastern part of the basin. To describe groundwater behavior and predict effects of management strategies, a three-dimensional, numerical model of groundwater flow in the Sujas aquifer was developed. Modeled water levels were most sensitive to the recharge rate, the horizontal hydraulic conductivity and the bottom layers. Observed water-level fluctuations were reproduced in some areas but not in other areas. Differences may be due to the influence of local-scale conditions not represented in the regional model or errors in parameterization of the aquifer data.

Key words: Groundwater, mathematical modeling, Sujas basin, MODFLOW, groundwater management

INTRODUCTION

The use of groundwater has been expanded worldwide. A serious threat to continued availability of this resource is contamination of human origin. Groundwater modeling has emerged as a powerful tool to help managers optimize use and as well as to predict the groundwater resources (Roscoe Moss Company, 1990). The complex problems related to functioning of groundwater system can be solved with the aid of models. Based on the principles involved in designing models can be classified as physical and mathematical model (Walton, 1970). Mathematical model can be used as a design tool. The flexibility of the method allows the flows mechanism to be explored and compared with wide variety of field information (Rushton and Redshaw, 1979). Extensive information must be provided before a model design. The information can be deduced from geological, geophysical, hydrological and other evidences. Useful text explaining these information are Fetter (1988), Todd (1980), Freeze and Cherry (1987), Bouwer (1978) and Davis and DeWeist (1966).

Mathematical model are further divided into analytical and numerical or digital model. In numerical models, the main numerical approaches used for solving groundwater equations are finite difference and finite element method. Both method requires that two regions of interest be subdivided using a mesh or grid network (Schwartz and Zhang, 2003). The reliability prediction using a groundwater model depends on the how the well the model approximates field situations (Anderson *et al*., 1992).

Several persons for example Cheng and Hodge (1976), Huyakorn and Pinder (1983), Frayer *et al*. (2001), Zheng and Bennett (1995) and Mirabzadeh and Mohammadi (2006) have developed solutions for water mass balance, solute and dispersion equation.

One of the most important points is to select groundwater modeling software which must possess selecting index like its capability, popularity and its friendly use (McDonald and Harbaugh, 1988).

Zanjan province of northwestern Iran can be perennially affected by scarcity of water if proper management is not followed. The problem is aggravated by the lack of productive surficial aquifers. In this study, lithologs from tube wells and Vertical Electrical Soundings (VES) have been used with other geologic information to identify aquifer horizons in the Sujas basin. The water table configuration, pattern of groundwater flow,

Corresponding Author: A. Taheri Tizro, Department of Water Engineering, Razi University, Kermanshah, Iran

hydraulic properties of shallow aquifers and groundwater quality were determined. Finally, a three-dimensional, finite-difference groundwater flow model was developed for the Sujas aquifer as a tool to improve our conceptual understanding of groundwater flow in the region; develop a management tool to support water planning and evaluate groundwater availability under drought conditions.

MATERIALS AND METHODS

Site description: The Sujas basin covers an area of 1298 km^2. The study area lies between latitudes 36°7′ and 36°30′ north and longitudes 48°16′ and 48°50′ east. The basin elevation ranges from 1650 to 2812 m above mean sea level. The study area is bounded by the Soltaniah Mountains to the north, the Agh Dagh and Alkhan Mountains to the east, the Ghidar Mountains to the south and the Ghare Dagh Mountains and Zarin Abad basin to the west. Ghidar is the only city in the area. The important villages in the area are Majid Abad, Zarand, Boulamchy, Mazid Abad and Yengejeh. Most of the area is rural and dependent on agriculture. Major crops include wheat, barley and peas. A few industries exist in the area (e.g., cement production).

Meteorological and hydrologic conditions: There are five meteorological stations in the area, two of which are synoptic. Average annual rainfall in this region recorded for the years 1968-2004 is about 350 mm. The rainfall contribution is 36% during spring (133.2 mm), 3% during summer (11.3 mm), 25% during autumn (92 mm) and 36% during winter (132.8 mm). The spring season occurs from April to June, summer from July to September, autumn from October to December and winter from January to March. The average minimum temperature is -3.7°C in February and the average maximum is 22.5°C in August. Relative humidity is highest in January and February (72%) and lowest in September. The total annual sunshine is 4449 h. Evapotranspiration was estimated by FAO-56 based upon Penman-Monteith equation Richard and Allen (1998). The average annual evapotranspiration rate calculated for a period of 30 years is 1044 mm. The entire catchment comes under the influence of Mediterranean fronts. According to the Demartin climatic classification, the region is semiarid. The Sujas River, which is perennial, is the main stream in the area. It originates mainly from northeastern catchments and flows westward for about 31 km in the basin. The mean annual discharge of the river at the Zarzar hydrometric station in the western part of the basin is about 0.75 Mm^3.

Geology: According to Nabavi (1979) and Stocklin (1986), the study area belongs to the central Iran tectonic zone. The area has been mapped by Geological Survey of Iran at a 1:1,250,000 scale and the geology has been described by Boulourchi (1979), Braud (1990), Zadeh (2002) and present studies. The northern rocks of the Sujas basin (Soltaniah Mountains) belong to the Alborz zone and the southern rocks (Ghidar Mountains) belong to the central Iran zone. The highest elevation in the basin (2812 m) is in the Ghidar Mountains. The border between the two zones in the central part of Sujas basin is marked by faulting.

The oldest rocks exposed in the area are Precambrian dolomitic limestones in the Soltaniah Mountains. The youngest rocks exposed are the Cenozoic upper red formations, which mainly consist of shale. The general strike of the rocks is north-northeast-south-southwest along the Alborz belt. The geology of the area is shown in Fig. 1 and the stratigraphic column is given in Table 1.

The Soltaniah Mountains, which extend for 30 km in length and 5-7 km in width, appear as a horst parallel to a major longitudinal fault. This range has been intensely faulted, particularly the northern part, so that Precambrian rocks overlie Tertiary rocks. Numerous traverse faults of various orientations disrupt the pre-Tertiary rocks into a complicated mosaic-like pattern.

The Ghidar Mountains form an anticline with axes oriented northwest-southeast and plunging gradually toward the NE. Diorites of Tertiary age are seen in the core of this anticline. This range has mostly been deformed by folding, but several transverse faults cut across structural trends.

The Pleistocene deposits in the Sujas basin, which are more than 250 to 300 m thick, have undergone quaternary faulting so that unconformities have appeared.

Hydrogeological setting: The occurrence of groundwater in the area is both structurally and stratigraphically controlled. In the northeastern, eastern and western parts of the basin, thick alluvial deposits constitute the aquifer-aquitard systems. Silt, sand and gravel deposits occur along the major river tributaries and include good aquifer horizons. In particular, point bars form good aquifers. Lithological data from exploratory wells show that the aquifer thickness increases from 25-40 m around the periphery of the basin to 120 m in the central part of the basin. Geological and geoelectrical studies have revealed the existence of a deeper aquifer overlain by thick, relatively impermeable Pleistocene beds in the western part of the basin. Only limited numbers of deep wells have been drilled in the area.

In the southern part of the basin, weathered and fractured rocks are likely to form aquifers. The existence of such aquifers is known due to recent drilling of a deep well.

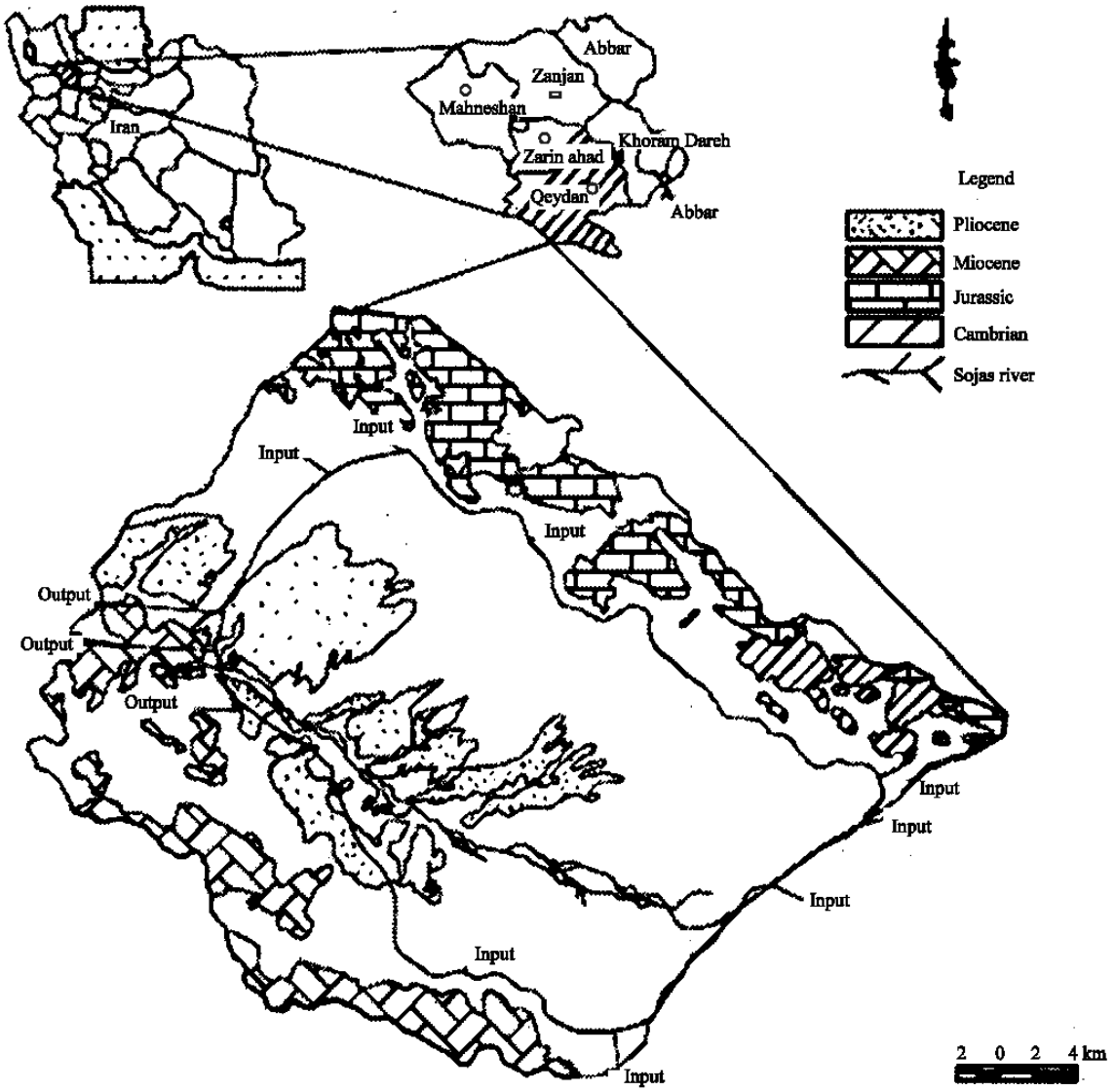

Fig. 1: Geological map of the area

Gently sloping horizontal wells (qanats) were dug through alluvial materials to lead water by gravity flow from beneath the water table at higher elevations to the ground surface outlets. There are 30 qanats discharging about 6.317 Mm^3 and 167 springs discharging 3.319 Mm^3 annually. There are 401 deep wells discharging 30.97 Mm^3 of groundwater annually. The discharge of wells ranges from 1 to 50 L sec^{-1}, with an average of 9.5 L sec^{-1}. These wells are mainly used for irrigation.

The depth to the water table is highly variable; it is relatively shallow in the central part and as deep as 50 m below ground level or more in northern parts. Groundwater flows from the recharge area of the upper hills toward the central part of the basin and ultimately discharges to the Sujas River or to wells. Transmissivity is of the order of 100 m^2 d^{-1} around the periphery and up to 2000 m^2 d^{-1} in the central part of the basin (Fig. 2). Specific yield ranges from 2 to 10%. Average discharge of the well is 9.5 L sec^{-1}.

Based on hydrograph analysis of observing well stations during the period 1997-2003, it is concluded that there is average decline of about 4 m in the static water level in the basin. Figure 3 shows the unit hydrograph of the basin.

Groundwater quality does not show any significant abnormality. The electrical conductivity ranges from 250 to 500 μmhos cm^{-1}. Maximum values of electrical conductivity occur in discharge areas, consistent with

Table 1: Stratigraphic succession

Age		Formation
Quaternary		
Holocene		Recent alluvium
Pleistocene		Terraces, gravel fans
Cenozoic		
Pliocene		Marl, silty clay, clay, shale (Upper red formation)
Miocene		Yellow to pink fossiliferous limestone (Qom formation)
Oligocene		Conglomerate (Lower red formation)
Tertiary eocene		Conglomerate and sandstone (Fajan formation)
Mesozoic		
Cretaceous	Upper	Phyllite, shale, volcanic rocks
Jurassic	Upper	Limestone with chert nodules (Lar formation)
	Lower	Sandstone and shale (Shemshak formation)
Paleozoic		
Permian	Upper	Limestone and sandy limestone (Ruteh formation)
	Lower	Sandstone, shale, quartzite (Doroud formation)
Cambrian	Upper	Dolimitic sandstone (Mila formation)
	Medium	Red sandstone (Lalun formation)
	Lower	Shale, sandstone, dolomite (Barut formation)
Pre cambrian		Dolomitic limestone, shale (Soltanieh formation)

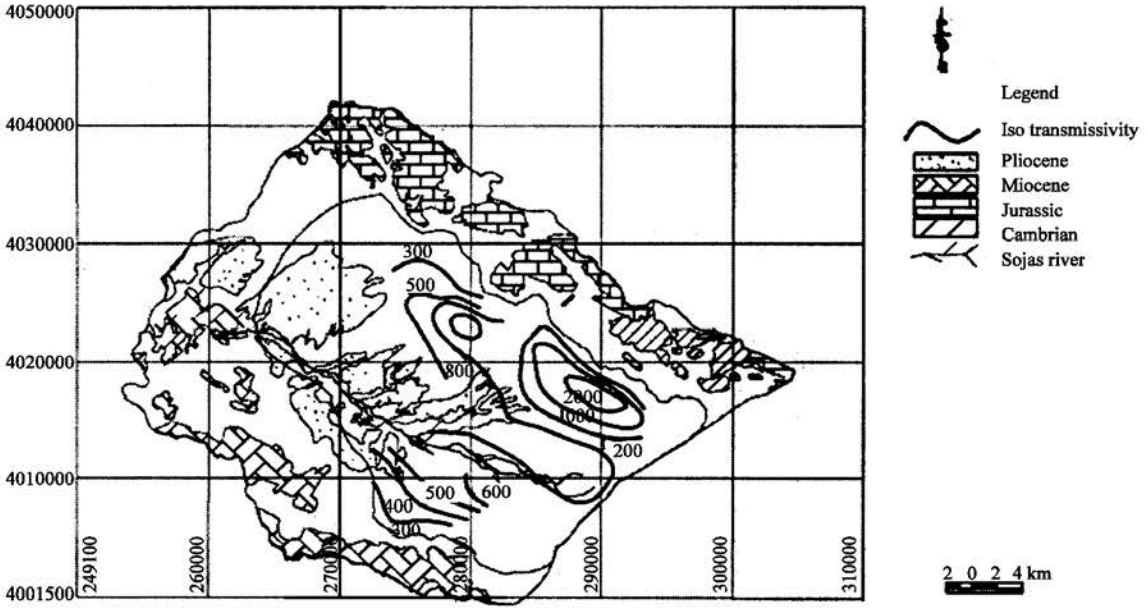

Fig. 2: Iso-transmissivity map

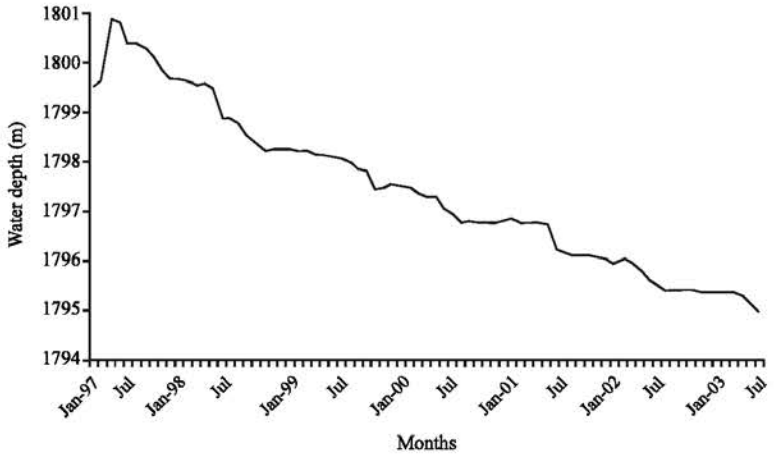

Fig. 3: Unit hydrograph of observation wells

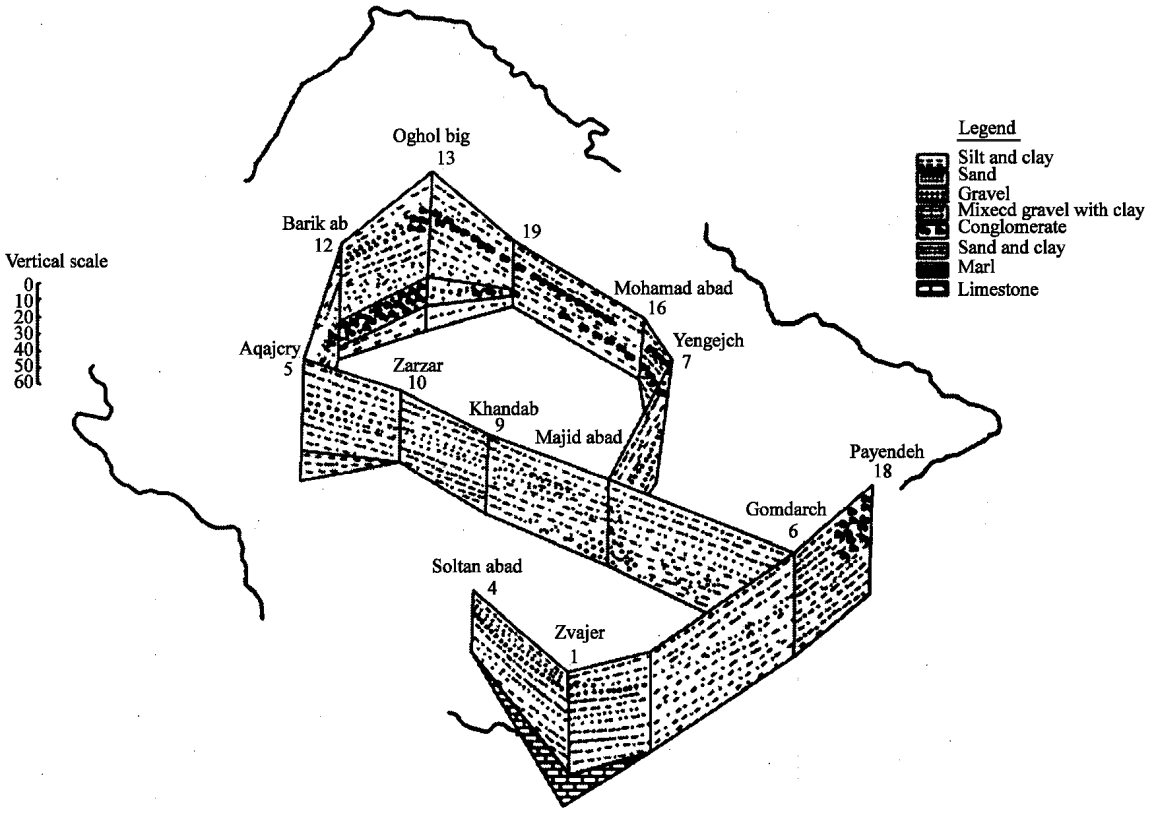

Fig. 4: Fence diagram of study area

progressive water-rock interaction along the groundwater flow paths. Total dissolved solids concentrations range from 208 to 1329 mg L^{-1}. In general, the groundwater is of bicarbonate type in recharge areas and sulfate concentrations increase in central parts of the basin. Further study of the controls on groundwater quality in the basin is needed.

Conceptual modeling: Developing a modeling concept is the initial and the most important part of every modeling effort. It requires a thorough understanding of hydrogeology, hydrology and dynamics of ground water flow in and around the area of interest. The result is a computerized database and simplified electronic maps and cross section that will be used in model (Kresic, 2006).

The available borehole data were used to understand: (1) the extent and boundaries of the aquifer, (2) recharge to and discharge from the aquifer, (3) water level fluctuations in the aquifer, (4) variations in the thickness and the depth of the aquifer and any confining strata, (5) spatial variations in transmissivity and storativity, (6) pumping test results, discharge and drawdown of wells, (7) possible river base flows, (8) spring location and spring flows and (9) other information related to the basic hydrogeology of the region, such as areas of interconnection between surface water and groundwater. A fence diagram (Fig. 4), which has been constructed from lithological data, illustrates the stratigraphic framework of the basin in quasi-three-dimensional form.

As the study of subsurface geology can often be made from lithological sections, fence diagram etc. which are prepared from available lithological data, limited availability of lithological data was difficult to study subsurface geology and severe constrains in compiling its holistic picture. These shortcomings were, however overcome by the use of geophysical data.

Geoelectrical measurements and interpretation: Vertical Electrical Soundings (VES) were conducted with a Schlumberger configuration in the area by Tamab (1968). For many locations new data were generated in the field. The apparent resistivity data obtained for different values of AB/2 have been processed. These results were subsequently used to obtain a realistic picture of the geological framework. Quantitative (indirect and direct) and geologic methods have been applied in the interpretation. Bhattacharya and Patra (1968) and Griffith and King (1965) have described the techniques used in

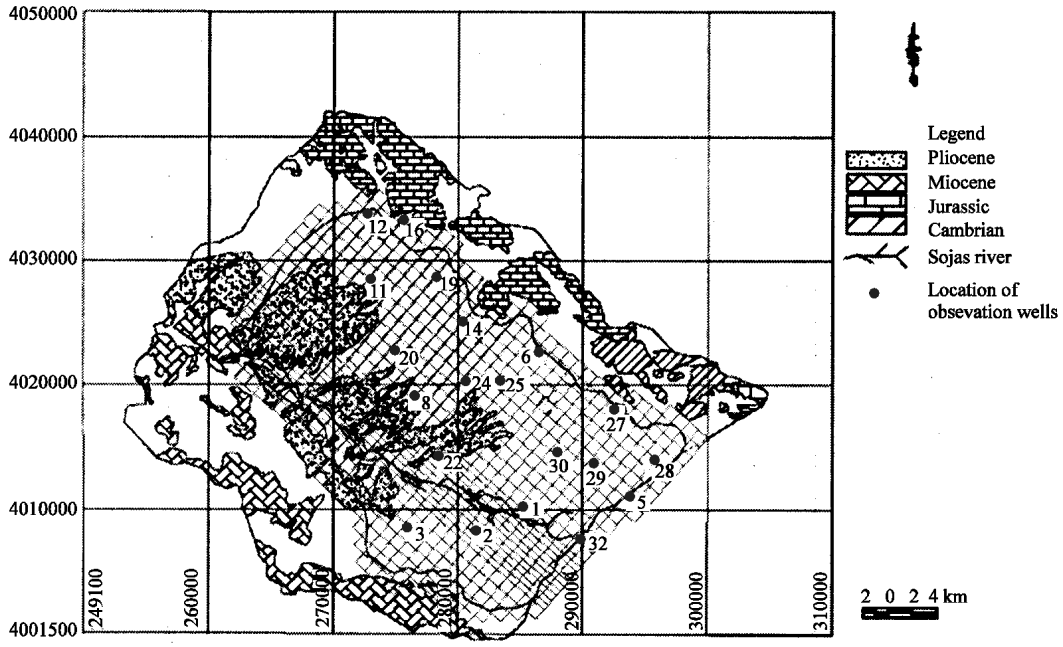

Fig. 5: Numerical model grid

the indirect interpretation. Comprehensive accounts of various approaches to automatic interpretation of resistivity data have been given by Zohdy *et al.* (1974), Zohdy (1989) and Niwas and Singhal (1983). Automatic interpretation of sounding data (Zohdy, 1989), which produces the interpreted depths and resistivities, respectively, has been utilized to obtain true resistivity values and the corresponding layer thicknesses.

The data have been carefully compared with the lithologs of boreholes located in the vicinity of the corresponding soundings. Resistivities for sandy horizons vary from 35-100 Ωm, whereas predominantly clay and silt zones show ranges of lower resistivity. The rock formations exhibit wider ranges of resistivity (150-400 Ωm). Low values of resistivity for these formations imply a friable and weathered nature.

Model design: The design of the model includes the choice of code and processor, the discretization of the aquifer into layers and cells and the assignment of model parameters. The model was designed to match the conceptual model of groundwater flow in the aquifer as much as possible.

MODFLOW-96 (Harbaugh and McDonald, 1996), a widely-used modular finite-difference groundwater flow code distributed by the US Geological Survey, was used. To obtain loading information into the model and observing model results, Processing MODFLOW for Windows (PMWIN) version 5.1 was used (Chiang and Kinzelbach, 1998).

The simultaneous equations used by MODFLOW for each finite difference cell is derived using Darcy's Law and the law of conservation of mass. The derivation gives a partial differential equation, which is used by MODFLOW. This partial-differential equation of groundwater flow used in MODFLOW is given as (McDonald and Harbaugh, 1988):

$$\frac{\partial}{\partial x}\left(K_{xx}\frac{\partial}{\partial x}\right)+\frac{\partial}{\partial y}\left(K_{yy}\frac{\partial}{\partial y}\right)+\frac{\partial}{\partial z}\left(K_{zz}\frac{\partial}{\partial z}\right)-W=S_s\frac{\partial h}{\partial t}$$

Where, K_{xx}, K_{yy} and K_{zz} are the values of hydraulic conductivity along the x, y and z coordinate axes, which are assumed to be parallel to the major axes of hydraulic conductivity. h is the potentiometric head W is the volumetric flux per unit volume representing sources and/or sinks of water, with W<0.0 for flow out of the ground-water system and W>0.0 for flow in. Ss are the specific storage of the porous material and t is time. This equation, when combined with boundary and initial conditions, describes transient three-dimensional ground-water flow in a heterogeneous and anisotropic medium, provided that the principal axes of hydraulic conductivity are aligned with the coordinate directions McDonald and Harbaugh (1988).

The lateral extent of the model corresponds to natural hydrologic boundaries, such as erosional limits, rivers and the structural and hydraulic boundaries to the west that coincide with groundwater divides. According to the

hydrostratigraphy and conceptual model, the model was designed to have one layer. IBOUND was defined by establishing the lateral extent of the formations in each layer using the geologic map. The IBOUND (Initial Boundary) array contains a code for this model cell which indicates whether (1) the hydraulic head is computed (active cell), (2) the hydraulic head is kept fixed at a given value (constant-head cell or time varying specified-head cell), or (3) no flow takes place within the cell (inactive cell). It was decided to use 1 for an active cell, -1 for a constant-head cell and 0 for an inactive cell. A cell was assigned as active if the formation covered more than 50% of the cell area. The model domain was discretized into grid dimensions of 1×1 km. smaller cells were assigned to the active model area where rivers, springs and abstractions are simulated. In total, the model contains 34 columns and 29 rows (Fig. 5).

The contouring program Surfer and the GIS program Arc view were used to infer distributed values of model parameters, including (1) elevations of the top and bottom of each layer, (2) horizontal and vertical hydraulic conductivity, (3) specific storage and (4) specific yield.

Boundary conditions for any groundwater flow model should reasonably reflect the physical system and be far enough removed from the primary model area to avoid interference. The model assigned boundaries for the parameters including (1) recharge, (2) pumping, (3) rivers, (4) springs, (5) outer boundaries and (6) initial conditions. Initial values for recharge were assigned using Arc view. A map of October 2000 water levels was used to assign initial heads for the steady-state model. The river package of MODFLOW was used to represent rivers and streams in the model. Outer-boundary conditions were assigned using the General Head Boundary (GHB) Package of MODFLOW, which requires values for hydraulic head and conductance, or assigned as constant-head.

RESULTS

Calibration of model in steady-state and transient conditions: The effectiveness of a groundwater model will depend on how accurately it has been calibrated. Data gaps in aquifer parameters and related information should be determined first. Steady-state calibration was attempted for water levels in the Sujas aquifer measured in October 2002, when pumping was expected to be lowest. Different model parameters were adjusted to determine which parameters had the greatest effect on simulated water levels. Through this initial sensitivity analysis, it was observed that the water levels in the Sujas aquifer were most sensitive to the recharge rate, the horizontal hydraulic conductivity and the bottom layers.

During the steady-state calibration, horizontal hydraulic conductivities, river-bed conductance and elevation of the bottom layer (depth to bedrock) were adjusted to achieve a good fit to observed water levels and satisfactory overall water balance for the model area. Figure 6 shows the depth of the bottom layer after

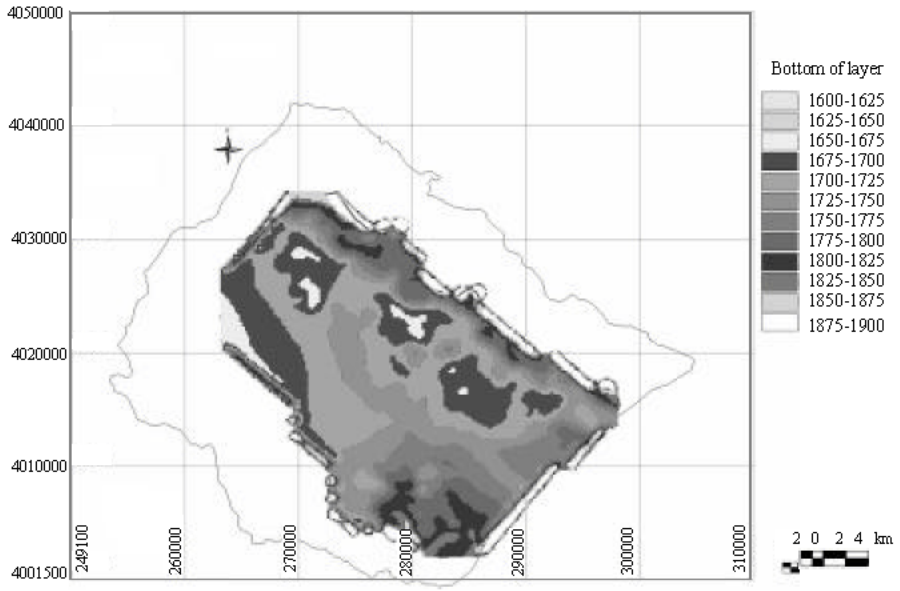

Fig. 6: Depth of bottom layer (Depth to bed rock)

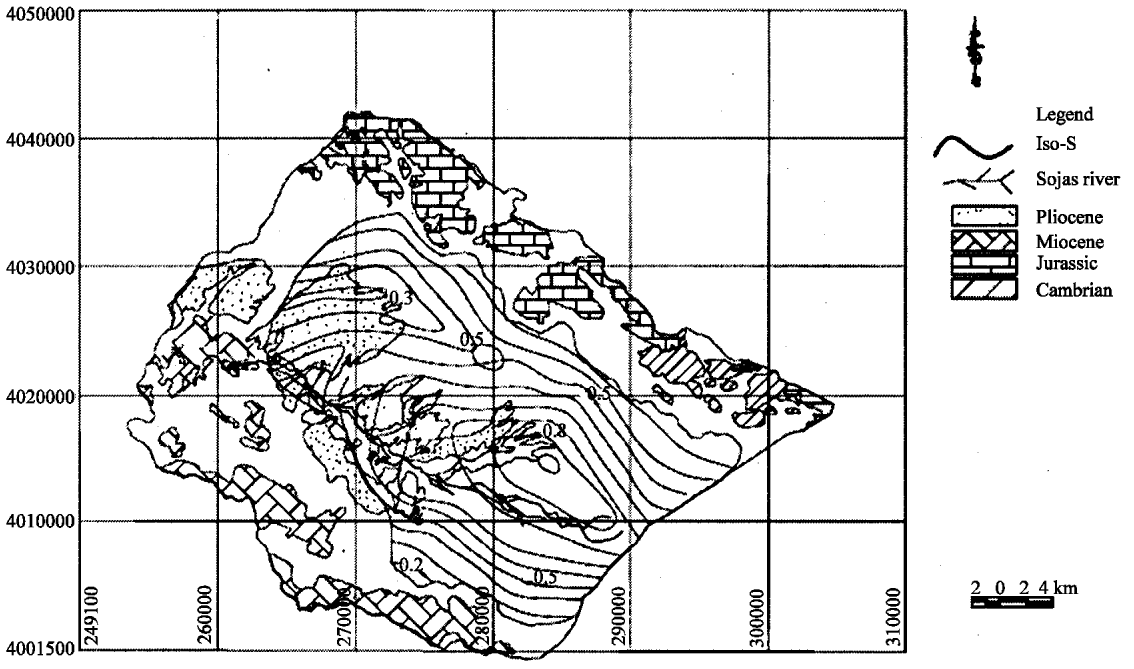

Fig. 7: Distribution of storage coefficient in study area

calibration. The transient model was developed based on the calibrated steady-state model. To transition from time-averaged steady-state conditions, the initial hydraulic heads for the transient model calibration were developed through the following iterative process. First, the final hydraulic heads for the steady-state model were applied as the initial heads for the transient model stress period (October 2002). The model was run for 12 stress periods, or months.

In the Sujas Basin the storage coefficients in primer stage was calculated manually, the calculated parameter was distributed among different cells of model by using GIS and other converter programs (Fig. 7).

The transient model calibration was optimized by trial-and-error adjustment of the storage coefficients for the model area. Specific storage and the layer thickness was used to calculate the confined storage coefficient.

Where calibrated values appeared to be improper, additional data were collected to refine the conceptual model. Figure 8 shows the distribution of observation wells in the study area.

For calibration of the transient model, water-level fluctuations resulting from recharge and pumping during 2002 and 2003 were simulated using monthly stress periods. Specific storage values were adjusted until the model approximately reproduced the range of water-level fluctuations observed in wells in the model area. The model matches observed water-level fluctuations well in some areas but not in others. Differences may be due to the influence of local-scale conditions not represented in the regional model or errors in our parameterization of the aquifer data. In general, however, the model does a good job of reproducing seasonal and annual water-level fluctuations in most wells and it accurately represents areas where water levels respond quickly to variations in recharge versus those where the water-level response is much more subdued. After calibration of model in unsteady condition, ground water in different time steps were computed. With regard to ground water balance was computed by model at first stress period, the aquifer storage shows increase to 3.68 Mm^3 and in second stress period with regard to start of abstractions of wells amount of aquifer recharge decrease to 16.8 Mm^3. Changes in the volume storage computed to be as -13.2 Mm^3.

Changes in water table depth of the aquifer calculated as:

$$\Delta h = \frac{\Delta V}{S \times A}$$

Where:

Δh = Changes in water table depth (m),
A = Area of the aquifer (m^2),
S = Average of storativity of aquifer and
ΔV = Changes in volume storage (m^3).

$$\Delta h = \frac{-13.2 \times 10^6}{0.368 \times 580.77 \times 10^6} = 0.61 \text{ m}$$

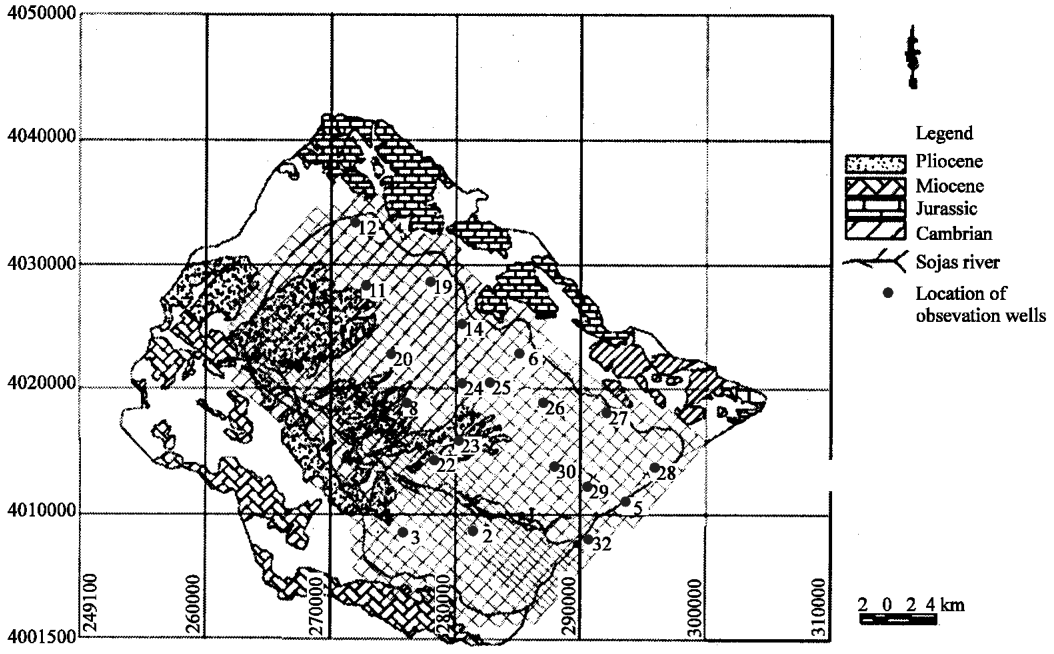

Fig. 8: Numerical model grid and observation wells

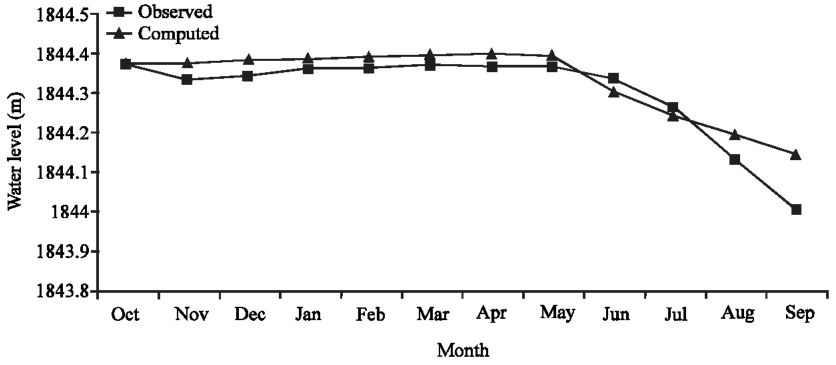

Fig. 9: Correlation between computed and observed values for transient simulation (well No. 2)

Therefore, there was an average decline of 0.61 m in the water table during the year.

Model verification for steady-state and transient conditions: Model verification involves using the calibrated model to simulate a hydrologic system that is known. In this study, verification involved comparing the calibrated water levels with the observed field data at different times. Figure 9 shows this comparison for well No. 2 in the transient simulation.

To assess the future availability of groundwater in the Sujas aquifer, the calibrated model was used to predict future water levels for three scenarios (dry, wet and normal). The time period for each scenario was six months with one-month (30 day) time steps. The model was run for a total of five years.

It was observed that, in the normal hydrologic period, the piezometers numbers 2, 8, 9, 11 have been impacted by perennial decline of ground water and other piezometers show seasonal fluctuations that emanate of difference in amount of recharge in hot and cold seasons. In the dry hydrologic period the most of piezometers show seasonal fluctuations of ground water and show decline in ground water table, but the piezometers numbers 14, 19, 20 have decline more than other piezometers, this part of aquifer will be encountered by perennial decline of ground water table this can be due to influence of local-scale conditions. In the wet hydrologic period, most of piezometers in central and northern of basin show slight rise in groundwater table, also the rate of declination of piezometers numbers 9, 22, 23 have been less.

CONCLUSIONS

Initial sensitivity analyses demonstrated that the water levels in the Sujas aquifer were most sensitive to the recharge rate, the horizontal hydraulic conductivity and the bottom layers. Transient simulations involved adjusting the values of the storage coefficient. The model matches observed water-level fluctuations well in some areas but not in others. Differences may be due to the influence of local-scale conditions not represented in the regional model or errors in parameterization of the aquifer data.

Ground water balance was computed by model at first stress period, the aquifer storage shows increase to 3.68 Mm^3 and in second stress period with attention to start of abstractions of wells amount of aquifer recharge decrease to 16.8 Mm^3. Changes in the volume storage computed to be as -13.2 Mm^3.

Changes in depth to water table of the aquifer were calculated as -0.61 m.

REFERENCES

Anderson, M.P., W.F. Mullican and W.W. Woessner, 1992. Applied Groundwater Modeling. Academic Press. San Diego, pp: 381.

Bhattacharya, P.K. and H.P. Patra, 1968. Direct Current Geoelectric Sounding. Elsevier, Amsterdam, pp: 139.

Boulourchi, 1979. Explanatory Text of Kabudar Ahang Quadrangle Map: Geological and Mineral Survey of Iran, pp: 65.

Bouwer, H., 1978. Groundwater Hydrology. McGraw -Hill Company Publication, pp: 480.

Braud, J., 1970. The Zagros formations in the region of Kermanshah. Bull. Soc. Geol. France (7), XIII, No. 3-4, 416-419 (In French).

Cheng, R.T. and D.S. Hodge, 1976. Finite element method in modeling geologic transport processes. Math. Geol., 8: 43-56.

Chiang, W.H. and W. Kinzelbach, 1998. Processing MODFLOW. A Simulation System for Modeling Groundwater Flow and Pollution. Software Manaul, pp: 325.

Davis, S.N. and R.J.M. Deveist, 1966. Hydrogeology. John Wiley and Sons Inc., New York, pp: 463.

Fetter, C.W., 1988. Applied Hydrogeology/Merrill Publishing Columbus, OH, pp: 592.

Frayer, A.E., W.F. Mullican and S. Macko, 2001. Groundwater recharge and chemical evolution in the southern high plains, USA. Hydrogeol. J., 9: 522-542.

Freeze, R.A. and J.A. Cherry, 1987. Groundwater. Prentice-Hall International, London, UK., pp: 524.

Griffith and King, 1965. Applied Geophysics for Engineers and Geologists. Paragon Press, London, UK., pp: 223.

Harbaugh, A.W. and M.G. McDonald, 1996. Programmer's documentation for MODFLOW-96, an update to the US geological survey modular finite-difference ground-water flow model: US Geological Survey Open File Report 96-486, pp: 220.

Huyakorn, P.S. and G.F. Pinder, 1983. Computational Methods in Subsurface Flow. Academic Press, New York, pp: 473.

Kresic, N., 2006. Hydrogeology and Groundwater Modeling. CRC Press, Taylor and Francis Group, New York.

McDonald, M.G. and A.W. Harbaugh, 1988. A Modular Three-Dimensional Finite-Difference Groundwater Flow Model. Techniques of Water Resource Investigations, 06-A1, USGS Publication.

Mirabzadeh, M. and K. Mohammadi, 2006. A dynamic Programming to solute transport and dispersion equations in groundwater. J. Agri. Sci. Technol., 8: 233-241.

Nabavi, 1979. Introduction to Geology of Iran. Geological Survey of Iran Publications, pp: 109.

Niwas, S. and D.C. Singhal, 1983. Aquifer transmissivity of porous media from resistivity data. J. Hydrol., 82: 143-153.

Richard, G. Allen, 1998. Crop evapotranspiration, guidelines for computing crop water requirements. FAO Irrigation and Drainage Paper 56 FAO-Food and Agriculture Organization of the United Nations, Rome.

Roscoe Moss Company, 1990. Handbook of Groundwater Development. John Willy and Sons Publication, pp: 467-474.

Rushton, K.R. and S.C. Redshaw, 1979. Seepage and Groundwater Flow. Numerical Analysis by Analog and Digital Methods. A Wiley-Interscience Publication. John Wiley and Sons, Ltd., New York, pp: 210-225.

Schwartz, F.W. and H. Zhang, 2003. Fundamentals of Ground Water. John Willey and Sons Publication, New York, pp: 574.

Stocklin, J., 1986. Structural history and tectonics of Iran: A review. Am. Assoc. Petroleum Geo. Bull., 52: 1229-1258.

Tamab, 1968. Geoelectrical Studies in Sujas Area. Water Resources Development Organization, Iran, pp: 210.

Tizro, A.T. and D.C. Singhal, 1993. Geoelectrical studies in Narnaul area for estimating transmissivity in alluvial aquifers. National Seminar on Hydrology, Roorkee, India.

Todd, D.K., 1980. Groundwater Hydrology. John Willey Sons. Inc., New York, pp: 535.

Walton, W.C., 1979. Progress in analytical groundwater modeling. J. Hydrol., 43: 149-159.

Zadeh, D., 2002. Geology of Iran. Amirkabir Publication, Tehran, Iran, pp: 600.

Zheng, C. and G.D. Bennett, 1995. Applied Contaminant Transport Modeling. Van No. Strand Reinhold, New York, pp: 440.

Zohdy, A.A.R., G.P. Eaton and D.R. Mabey, 1974. Application of Surface Geophysics to Ground-Water Investigations: Techniques of Water-Resources Investigations. Chapter, Book 2, USGS Publication, D1, pp: 116.

Zohdy, A.A.R., 1989. A new method for automatic interpretation of Schlumberger and Wenner sounding curves. Geophysics, 54: 245-253.